Computer Methods in Biomechanics and Biomedical Engineering: Imaging & Visualization

ISSN: (Print) (Online) Journal homepage: www.tandfonline.com/journals/tciv20

Non-invasive and non-contact automatic jaundice detection of infants based on random forest

Fatema-Tuz-Zohra Khanam, Ali Al-Naji, Asanka G. Perera, Danyi Wang & Javaan Chahl

To cite this article: Fatema-Tuz-Zohra Khanam, Ali Al-Naji, Asanka G. Perera, Danyi Wang & Javaan Chahl (2023) Non-invasive and non-contact automatic jaundice detection of infants based on random forest, Computer Methods in Biomechanics and Biomedical Engineering: Imaging & Visualization, 11:6, 2516-2529, DOI: 10.1080/21681163.2023.2244601

To link to this article: https://doi.org/10.1080/21681163.2023.2244601

Published online: 20 Aug 2023.

COMPUTER METHODS IN BIOMECHANICS AND BIOMEDICAL ENGINEERING: IMAGING & VISUALIZATION
2023, VOL. 11, NO. 6, 2516–2529
https://doi.org/10.1080/21681163.2023.2244601

Non-invasive and non-contact automatic jaundice detection of infants based on random forest

Fatema-Tuz-Zohra Khanam[a], Ali Al-Naji[b], Asanka G. Perera[c], Danyi Wang[a] and Javaan Chahl[a,d]

[a]STEM, University of South Australia, Mawson Lakes, Australia; [b]Electrical Engineering Technical College, Middle Technical University, Baghdad, Iraq; [c]School of Engineering and Information Technology, University of New South Wales, Canberra, Australia; [d]Platforms Division, Defence Science and Technology Group, Edinburgh, Australia

ABSTRACT

Jaundice is a common phenomenon in neonates and a significant cause of morbidity and mortality. Early detection of jaundice is still a significant challenge. Moreover, existing invasive techniques are stressful, and painful for the newborn, and non-invasive devices are expensive. Therefore, we investigate the characteristics of a non-invasive and non-contact neonatal jaundice detection system based on skin colour analysis and machine learning using a graphical user interface (GUI). First, we automatically selected a region of interest (ROI) from the image of an infant captured by a digital camera. Then, the skin colour of the selected ROI was analysed in both RGB and YC_bC_r colour spaces. Finally, a machine learning algorithm based on random forest (RF) was incorporated to classify jaundice or normal and determine whether the neonate requires treatment or not. The experimental result demonstrates that the proposed jaundice detection system has the potential as a non-invasive technique in clinical application.

ARTICLE HISTORY
Received 24 February 2023
Accepted 28 July 2023

KEYWORDS
neonatal jaundice; bilirubin; automatic ROI selection; skin colour analysis; machine learning

1. Introduction

Neonatal jaundice is a common disease found in newborn infants in their first few weeks of life (Gartner 1994; Katti and Babu 2021). According to worldwide statistics, 80% of preterm infants and 60% of term newborns, and 10% of breastfed newborns were prone to neonatal jaundice (Rennie et al. 2010). Every year total of 24 million newborns get jaundiced (Padidar et al. 2019).

Jaundice or hyperbilirubinemia is defined as the yellow discoloration of the skin and sclera of the eyes due to an excess level of bilirubin (Dzulkifli et al. 2018). Generally, jaundice is noticeable when serum bilirubin level exceeds 2.0 mg/dl in the blood (Puppalwar 2012). Bilirubin is a water-soluble tetrapyrrolic yellowish pigment that is present in the blood and whose excess accumulation in the skin results in neonatal jaundice symptoms (Ansong-Assoku and Ankola 2018). Bilirubin is created due to the breakdown of old red blood cells. In the human body, new red blood cells are produced, and old ones are broken down continuously. In an adult, the red blood cells survive for about 120 days; however, in a newborn infant, they survive for a significantly shorter time. Hence, newborns have higher than average quantities of red blood cells, which leads to excess bilirubin level due to the breakdown of more red blood cells (Ansong-Assoku and Ankola 2018). Normally, the damaged blood cells that produce bilirubin are metabolised by the liver for excretion. Later, bilirubin is secreted through urine and bile (Chee et al. 2018). Short-term excess of bilirubin is mostly harmless and self-limiting. But a high level of bilirubin in newborn infants is neurotoxic and can permanently damage the brain, which is called kernicterus. It may cause cerebral palsy, deafness or hearing loss, language difficulties, and developmental delay or can be fatal in the worst cases (Ullah et al. 2016; Chee et al. 2018).

Kernicterus can be avoided by early detection and treatment of jaundice or hyperbilirubinemia. High bilirubin can be controlled through phototherapy, a method that requires exposure of the affected newborn infant to particular wavelengths of blue light that transform bilirubin into a harmless, excretable form (Maisels 2015; Mreihil et al. 2018). On the other hand, excess bilirubin may need to be removed through Exchange transfusions (ET) in cases of extremely high levels (Women's NCCf, Health Cs 2010). However, ET is an invasive technique where a calculated amount of the newborn's blood is replaced by a donor's blood to decrease the excess level of bilirubin. Therefore, phototherapy has been the most popular method for the treatment of jaundice or hyperbilirubinemia (Mreihil et al. 2018; Katti and Babu 2021).

For detecting jaundice, there are different invasive and non-invasive approaches (Dzulkifli et al. 2018). Total Serum Bilirubin (TSB) measurement is a common invasive technique to determine the level of hyperbilirubinemia that works based on spectrophotometry using a small blood sample taken by a syringe and needle (Deepthi et al. 2019). However, the TSB measurement can be performed only by medical experts with good facilities. Moreover, as it is an invasive technique, this procedure is stressful for both infants and parents (Aydın et al. 2016). For the diagnosis of jaundice, there are some other techniques that involve the collection of blood samples.

CONTACT Fatema-Tuz-Zohra Khanam fatema-tuz-zohra.khanam@mymail.unisa.edu.au STEM, University of South Australia, Mawson Lakes 5095, Australia

Nevertheless, all invasive procedures are uncomfortable and painful for the infant, have a risk of infections, may cause anaemia, and will create anxiety for parents (Singla and Singh 2016).

Visual assessment is the simplest, non-invasive approach to identify hyperbilirubinemia in newborns (Shafiq et al. 2019). However, as this process is operator-dependent and may be affected by the skin colour of the infant, this process is not reliable for detecting jaundice (Riskin et al. 2008; Keren et al. 2009). On the other hand, Transcutaneous Bilirubinometry (TcB) is a non-invasive alternative technique to TSB measurement, which can reduce blood sampling by approximately 30% (Mansouri et al. 2015). Still, TcB techniques are expensive as they require products that have a huge recurrent cost. Moreover, The TcB test can be performed on babies who are 35 weeks or more of gestation age and 24 hours after birth (Mussavi et al. 2013). Therefore, in the case of infants who are born before 35 weeks of gestation as well as in the first 24 hours after birth, TcB is ineffective.

With the development of new advanced technologies such as smartphones and digital cameras, there is the possibility of a more efficient, cost-effective, and portable system to monitor jaundice. These new technologies may perform equivalently to existing monitoring tools, while being affordable and available (Srividya et al. 2022). Most of these methods have used image processing and colour analysis for jaundice detection (Osman et al. 2014).

In the literature, different jaundice detection systems were proposed based on computer vision and image processing techniques (Hashim et al. 2021). Different systems used different objects, such as skin colour (Hashim et al. 2021), sclera colour (Laddi et al. 2013), urine strips (Gupta et al. 2015) and stool (Angelico et al. 2021) for the colour analysis process. However, using urine strips and stool is not feasible as it is difficult to collect urine and stool. Moreover, these systems are not reliable and accurate as the colour of urine and stool may be affected by food (Hashim et al. 2021).

Some researchers have considered sclera colour to detect jaundice. For example, Laddi et al. (2013), proposed a non-invasive, low cost and instant jaundice detection method using the images of sclera of the eyes captured by a 3CCD colour camera. The authors used multiple image-processing techniques, such as image segmentation, image morphology, and colour analysis. Principal component analysis (PCA) was used to differentiate between jaundice and non-jaundice patients. Finally, an adaptive neuro-fuzzy inference system (ANFIS) algorithm was incorporated to measure jaundice and its degree of severity. However, the eyes of the babies remain closed most of the time, and to take the image of sclera, the head needed to be in a fixed position which is difficult to attain with infants. Hence, the proposed approach is more appropriate for adults rather than infants. Moreover, the accuracy of the proposed method depends on the training data to a great extent. Miah et al. (2019), introduced another non-invasive system for jaundice detection and bilirubin level quantification by capturing the image of the sclera using a webcam and a controllable LED flashlight. They selected ROI automatically using colour thresholding and bounding box algorithms. Furthermore, to estimate the bilirubin level, different machine learning-based regressions such as decision tree regression, linear regression, k-NN regression, SVM regression, and RF regression were used. Among all, RF regression gave the best results, with an absolute mean error of 0.29. The proposed technique was able to identify jaundice and deliver results within 5 minutes. Furthermore, to operate the system, no trained person was required. However, the system required the subject to wear specially-made goggles and a controlled lighting system, and it was only suitable for adults.

For detecting neonatal jaundice, using sclera colour is not feasible as it is difficult to capture the image of an infant's eyes due to the amount of time, they spend sleeping and unpredictable movements. Furthermore, for capturing the image of the sclera, participants need to maintain a controlled posture which is not possible for infants. Moreover, some infants' sclera may have a blue hue as they are thinner than adult sclera.

Skin colour is one of the common indicators that has been used for detecting jaundice, especially in the case of neonates (Amani et al. 2019). For instance, Aune et al. (2020), presented a physics-based system to measure bilirubin from digital images of newborn babies using a smartphone and a colour calibration card. In the proposed system, the authors undertook a combination of colour analysis of digital photographs and a physics-based model of transportation of light in the skin. A library of simulated reflectance spectra of skin was created by means of a mathematical model using diffusion theory. However, they mainly considered Caucasian-term infants as participants in their study and used manual ROI selection.

Hashim et al. (2021), developed a diagnosis and treatment process for neonatal jaundice based on infants' skin colour analysis using a digital camera and MATLAB graphical user interface (GUI). The system proposed in (Hashim et al. 2021) has two key sections: skin colour analysis and the practical circuit. The first one included manual ROI selection and colour range selection. On the other hand, the practical circuit was designed employing the Arduino Uno Microcontroller that was linked with the MATLAB GUI panel. However, in the proposed method (Hashim et al. 2021), the ROI was selected manually, and the sample size was very small, as they considered only two infants. Moreover, they only considered controlled lighting. In (Hashim et al. 2021), the authors considered 20 infants with varying skin tones, different lighting conditions and camera distance. In the proposed system, different image processing techniques were considered, such as skin detection based on colour space transformation and threshold value, automatic ROI selection using a bounding box algorithm, skin colour analysis in RGB and YC_bC_r colour spaces. The values of the B and Cb channels were compared with the predefined threshold value in order to determine whether the neonate had jaundice or not. The system provided the treatment of jaundice as well by employing an Arduino Uno microcontroller which controlled a blue LED light that provided phototherapy. However, the selected ROI included background pixels which may affect the results.

Moreover, they only considered values of the B and C_b channel to detect jaundice.

Kawano et al. (2018), proposed a non-contact and non-invasive neonatal jaundice detection method using a video camera and 8-colour calibration card based on skin colour analysis. They first detected the face automatically by using a cascaded object detector and then extracted the face skin region by removing the feature map, which was a combination of a mouth map and eye map from the detected face region. Two image features were used to detect jaundice: the mean value of skin colour information and eigenvalues of the variance-covariance matrix. However, the proposed skin detection technique could not extract skin regions clearly, as eyes and eyebrows might not be separated using an eye map. As a result, there were some failure cases, especially in the case of premature babies. Therefore, local areas, such as the forehead and cheek in the face, need to be detected to get better results. Moreover, the calibration card needed to be discarded after every use and changed to a new one before every use to prevent the possibility of infection of the infant, which requires an additional consumable expense.

Machine learning has great potential in medical applications, especially in detecting jaundice and measuring the level of bilirubin. For example, Rong et al. (2016), introduced an automated image-based (AIB) system that used an automated smartphone and a colour calibration card to detect jaundice. The images of skin taken by the smartphone had been uploaded to a cloud server that used machine learning-based software to deliver an immediate and individualised estimated bilirubin index. The results were compared with TSB and TcB for both term and preterm babies and showed a good correlation and strong relevance between AIB and TSB. However, the specificity and sensitivity of the proposed scheme were not good enough. Moreover, they used manual ROI selection.

Chakraborty et al. (2020), proposed a non-invasive system for detecting neonatal jaundice based on the yellowness of skin using a Raspberry Pi microcontroller and Pi camera. They used different image processing techniques and Convolutional Neural Networks (CNN) to detect jaundice. However, CNN has high computational complexity and is thus time-consuming. Castro-Ramos et al. (2014) introduced the detection of jaundice in adults or newborns using digital images from a smartphone. They considered RGB attributes as well as diffuse reflectance spectra acquired from a spectrometer as the factor to distinguish whether subjects had jaundice or not. A support vector machine (SVM) was used to distinguish between sick and healthy subjects. However, they only considered Mexican patients as their subject. Moreover, the specificity and sensitivity of the system were not adequate.

Juliastuti et al. (2019), estimated the risk zone of jaundice in newborn infants based on skin colour analysis using a digital camera. First, the image of a baby was filtered and colour-corrected using a median filter and a colour card, respectively. Then, baby skin was obtained by segmenting the image using a K-Means segmentation method. Finally, bilirubin level was estimated using multivariable linear regression. The proposed method was simple and had good correlation with TSB; however, the error percentage and accuracy of the system were only 17% and 67%, respectively. Moreover, they selected the ROI manually.

De Greef et al. (2014) developed BiliCam, a new non-invasive and low-cost system for monitoring jaundice in newborns using a smartphone camera (iPhone 4S) based on skin colour. The algorithm includes colour balancing, feature extraction and different machine learning-based regressions such as least angle regression (LARS), LARS-Lasso Elastic Net, k-NN regression, support vector regression (SVR), and RF regression. However, in the proposed system, a colour calibration card was required to be placed on the neonate's forehead and sternum before capturing the images. Moreover, they used manual ROI selection. The technique may also be constrained by skin tone especially darker complexion, body position and unclear ROI. In another study, Mansor et al. (2011), proposed a non-invasive method of detecting the jaundice of newborns using principal component analysis (PCA) based feature extraction and K nearest neighbour (k-NN) algorithm. They used the Intel Open CV cascade Classifier developed by Viola and Jones (2004) to detect the face. However, the detected face also contains background pixels which may affect the results of jaundice detection.

Most of the non-invasive systems in the literature used manual ROI selection. Few of them used automatic ROI selection techniques; however, the existing ROI selection techniques detected the whole face which included areas such as mouth, eyes, nostril, clothes and background, which may affect the results of jaundice detection.

Jaundice detection is a real-time requirement, and the entire procedure becomes ineffective when the ROI selection is not automated. Moreover, the reliability of jaundice detection depends on selecting the correct skin ROI of the infant. Selecting the entire face might not be the best ROI as it can include undesirable areas such as the mouth, eyes, nostril, clothes, and background. Therefore, we selected an ROI automatically from the infant's forehead.

In this paper, a non-invasive and non-contact neonatal jaundice detection system based on skin colour analysis and machine learning was proposed to minimise the limitations of existing invasive methods. First, we have designed an automatic ROI selection technique, including face detection, face landmark detection and ROI i.e. forehead selection. Then, skin colour was analysed in both RGB and YC_bC_r colour spaces for the selected area. Finally, jaundice has been detected using a machine learning algorithm based on RF. Moreover, the conceptual system could notify whether the neonates require phototherapy or not based on the outcome, demonstrated through a MATLAB GUI panel. The experimental result indicates that the proposed jaundice detection system has the potential as a non-invasive application of jaundice detection in the health sector.

The main contribution of this paper is the development of an automatic ROI selection technique as an advance over existing techniques using manual ROI selection. Moreover, we considered the infant's forehead as the ROI rather than the entire face. Furthermore, we used a machine learning algorithm to classify jaundice or normal to increase the reliability of the system.

Different Machine Learning Algorithms are introduced in section 2. Methods and materials, including data collection and

the system framework, are explained in section 3. Then, in section 4 and 5, the experimental results are represented and discussed, respectively. Finally, this work concludes with the key findings, limitations, and future research directions in section 6.

2. Machine learning algorithms

2.1. Naive Bayes

Naive Bayes (Hastie et al. 2009) is a probabilistic classifier based on Bayes' theorem. It assumes that features are conditionally independent given the class label. It is computationally efficient, especially for high-dimension data, and it can handle both categorical and numerical features. It performs well with small training datasets and is relatively robust to irrelevant features. However, Naive Bayes assumes independence between features, which may not hold, leading to suboptimal performance.

2.2. K-Nearest neighbours (KNN)

KNN (Han et al. 2012) is a non-parametric, instance-based learning algorithm that classifies new instances based on the majority class of its k nearest neighbours in feature space. It is simple to understand and implement, and it can handle both classification and regression tasks. It is a lazy learning algorithm, which means it does not require explicit training. The training phase only involves storing the training data. KNN can be sensitive to the choice of the k value, the distance metric, and feature scaling. It can also be computationally expensive, especially with large datasets.

2.3. Support vector machine (SVM)

SVM (Bishop and Nasrabadi 2006) is a supervised learning algorithm that finds an optimal hyperplane to separate the data into different classes while maximising the margin between the classes. SVM can handle both linear and non-linear classification tasks through the use of different kernel functions. It is effective in high-dimensional spaces and can handle datasets with a small number of samples. SVM can be sensitive to the choice of the kernel and the regularisation parameter, and it may not perform well on noisy datasets or those with overlapping classes.

2.4. Decision tree

Decision Tree (Mitchell 2007) is a flowchart-like model that makes predictions by partitioning the feature space based on feature values and learning simple decision rules. Decision Trees are interpretable and can handle both categorical and numerical features. They can capture complex relationships and interactions between features. They are prone to overfitting, especially with deep or complex trees, and they may not generalise well to unseen data. They are computationally efficient during both training and prediction.

2.5. Random forest (RF)

RF (Mitchell 2007) is an ensemble learning method that combines multiple decision trees to make predictions. Each tree is trained on a random subset of the training data and a random subset of features. Random Forest reduces over-fitting by aggregating the predictions of multiple trees, improving generalisation, and increasing model robustness. It can handle high-dimensional data, measure variable importance, and handle both classification and regression tasks. Random Forests can be slower to train and make predictions compared to single decision trees due to the ensemble approach.

2.6. Stochastic gradient boosting (SGB)

SGB (Friedman 2020) is an ensemble learning method that combines weak learners, typically decision trees, through sequential model building. It iteratively fits weak learners to the negative gradient of the loss function, minimising the loss and improving predictions at each step. It tends to produce more accurate predictions compared to single decision trees or Random Forests and can handle complex relationships in the data. However, SGB can be computationally expensive and sensitive to hyperparameter tuning. It requires careful optimisation and can be prone to overfitting if the number of boosting iterations is too high.

3. Methods and materials

The proposed method consists of simulated and real image data collection for the experiments, analysing facial region for the custom ROI, image feature extraction and jaundice detection.

3.1. Data collection

Two different datasets were used to test the functionality of the proposed system. The first data was obtained by creating 20 images of 3D babies with varying skin tones. These images were used as an alternative to real babies for investigating four different scenarios. The first scenario is for images that have typical light skin representing infants without jaundice. On the other hand, the second scenario is for images that have yellowish light skin representing infants with jaundice. The third scenario is for images that have normal brown skin that shows brown skin infants without jaundice, and the fourth scenario is for images that have a yellowish-brown skin colour that shows brown skinned infants with jaundice.

The second data set contains 30 images of babies taken from the internet; 20 of these images are for healthy infants without jaundice, and the other 10 images are for infants with jaundice. Collecting our own jaundice dataset from real patients was challenging and time-consuming. Therefore, we selected suitable images from the internet for this study.

3.2. System framework

As shown in Figure 1, the overall system includes various techniques such as automatic ROI selection, skin colour analysis, feature extraction and jaundice detection.

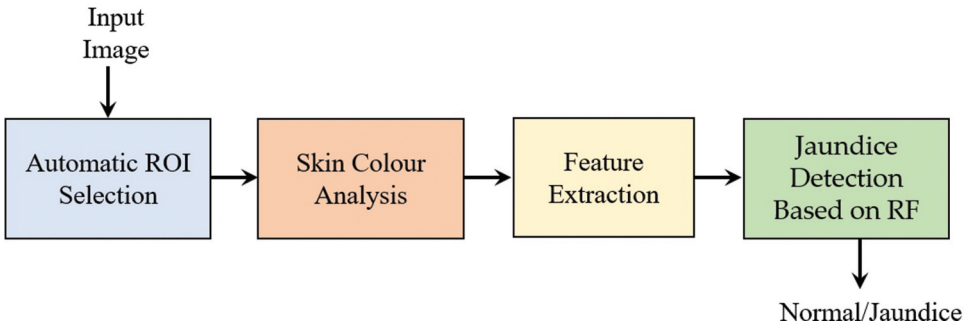

Figure 1. Block diagram of the proposed system.

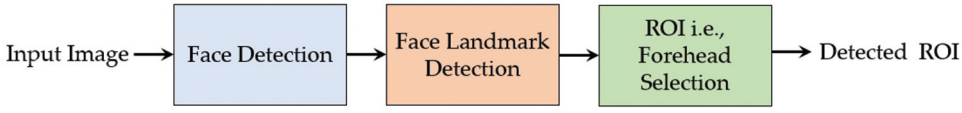

Figure 2. Block diagram of automatic ROI selection.

3.2.1. Automatic ROI selection

The reliability of jaundice detection depends on selecting the correct skin ROI of the infant. Selecting the entire face might not be the best ROI as it can include undesirable areas such as the mouth, eyes, nostrils, clothes, and background. Therefore, we selected an ROI from the infant's forehead. As shown in Figure 2, The ROI selection algorithm consists of three parts, namely face detection, face landmarks detection and ROI, i.e. forehead selection.

For face detection, we used Dlib library's (King 2009) HOG (Histogram of Oriented Gradients) and linear SVM (Support Vector Machine)-based face detector. This face detector is faster compared to a convolutional neural network (CNN)-based method. As the babies are in proximity to the camera, their faces are clearly visible in the images. Therefore, both CNN and HOG-based methods detect the faces accurately. CNN is state-of-the-art in face detection, but considering the processing speed, we use the HOG-based detector here. By nature of how the HOG descriptor performs, it is not invariant to variations in viewing angle and rotation.

Next, we detected 68 facial landmarks on the detected face. The landmarks are the jawline, eyebrows, eyes, nose bridge, lower nose, outer lip and inner lip. We experimented with different ROIs in the face and determined that forehead ROI was more reliable for our experiments. The geometry of the forehead helps to obtain a consistent skin ROI. The other areas of the face are more susceptible to shadows and inconsistent lighting.

In order to analyse the skin of the baby, a suitable area should be selected. The face is the most visible part of the body of infants in a healthcare setting. Commonly used face detection techniques include detecting the whole face as bounding box or segmenting the face area. These techniques do not provide an ROI with a skin area suitable for jaundice detection. As the colour difference between jaundice positive skin and normal skin can be subtle, a carefully selected skin area helps improve the accuracy. Based on the shape of the face, the forehead is the most suitable area for a skin analysis task. To accurately select an ROI from the forehead, we used the facial landmarks. The landmark-based ROI selection avoids distracting and colour contrasting areas such as the eyes, nostrils, mouth, and the background.

The ROI bounding box was created using the eyebrow landmarks. The mid-points of the eyebrows were moved towards the forehead by a constant pixel distance h. We calculated h by scaling down the distance between the eyes. The bounding box was oriented roughly at the middle of the forehead. The jaw line, the raised eyebrow points, and the bounding box for three infant images are shown in Figure 3. The ROI selection algorithm is presented in Figure 4.

3.2.2. Skin colour analysis

After selecting ROI, we need to do the skin colour analysis. In numerous human-related image processing applications, skin colour is a very informative parameter (Chen et al. 2003, Vezhnevets et al. 2003; Kakumanu et al. 2007; Khanam et al. 2022). In skin colour detection, skin-coloured regions and pixels are identified in each image using three main colour spaces: RGB (Red, Green and Blue), YC_bC_r (Luminance, Chrominance) and HSV (Hue, Saturation and Value). The RGB representation of the brightness values variations can be obtained using the following equations (mTkalcic and Tasic 2002; Tkalcic and Tasic 2003)

$$R = \int E_\lambda R_\lambda d(\lambda), \tag{1}$$

$$G = \int E_\lambda G_\lambda d(\lambda), \tag{2}$$

$$B = \int E_\lambda B_\lambda d(\lambda), \tag{3}$$

where $E_\lambda$is the light spectrum, λ is the wavelength of the incident spectrum, and $R_\lambda, G_\lambda and B_\lambda$are the sensitivity functions for the R, G and B channels acquired from the colour image, respectively. The colour representation of the YC_bC_r colour

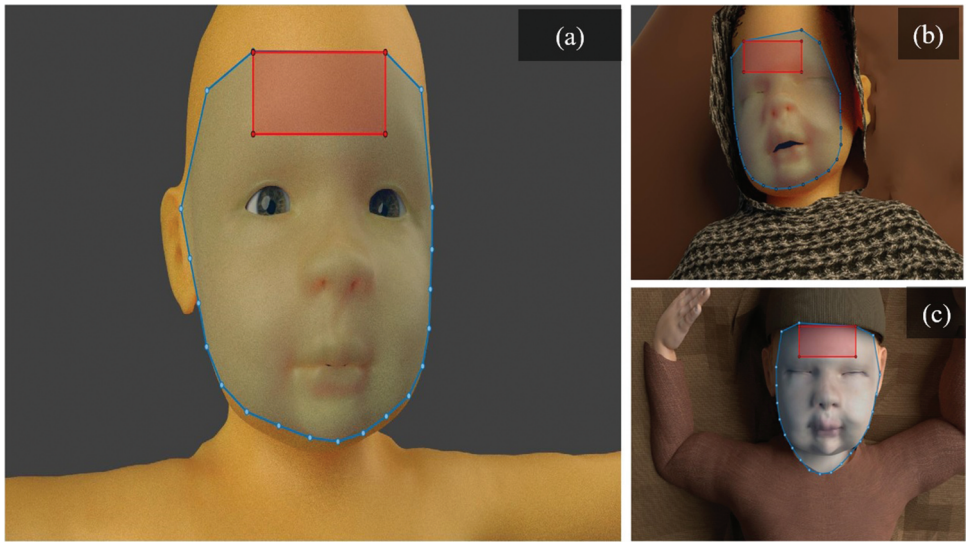

Figure 3. Automatic ROI selection. (a) the infant is in a straight position. (b) the infant with a tilted head. (c) the infant wearing a cap.

Algorithm 1: ROI selection

Input: image_frame
Output: ROI_pixels

```
Function face_detector(image_frame):
    return face_bounding_box
Function face_landmark_detector(image_frame,
  face_bounding_box):
    return face_landmarks
Function Main:
    face_detector(image_frame)
    face_landmark_detector(image_frame, face_bounding_box)
    select two middle forehead landmarks (f1,f2)
    set the ROI width and height w.r.t. (f1,f2)
    select the ROI pixels from image_frame
    return ROI_pixels
```

Figure 4. Algorithm of ROI selection.

space can be obtained from the RGB colour space using the following equation (Kumar et al. 2016)

$$\begin{bmatrix} Y \\ C_b \\ C_r \end{bmatrix} = \begin{bmatrix} 16 \\ 128 \\ 128 \end{bmatrix} + \begin{bmatrix} 0.279 & 0.504 & 0.098 \\ -0.148 & -0.291 & 0.439 \\ 0.439 & -0.368 & -0.071 \end{bmatrix} \begin{bmatrix} R \\ G \\ B \end{bmatrix} \quad (4)$$

An excess level of bilirubin creates a yellow discoloration of the skin. We transformed the original RGB colour space into the YC_bC_r colour spaces in order to better observe this subtle discoloration.

3.2.3. Feature extraction

We calculated the mean values for each colour channel of RGB and YC_bC_r colour spaces, resulting in 6 features.

The mean value of the brightness pixel for R, G, B channels within the selected ROI can be calculated as follows

$$F_R, F_G, F_B = \frac{\sum_{x,y \in ROI} I(x,y)}{|ROI|} \quad (5)$$

where $|ROI|$ is the size of the selected ROI, and $I(x,y)$ is the brightness pixel value at image location (x,y) for R,G,B channels. The value of Equation (5) ranges between 0 and 255.

Within the selected ROI, the mean value of the brightness pixel for Y, C_b , C_r channels can be measured as follows

$$F_Y, F_{C_b}, F_{C_r} = \frac{\sum_{x,y \in ROI} I(x,y)}{|ROI|} \quad (6)$$

where $|ROI|$ is the size of the selected ROI and $I(x,y)$ is the brightness pixel value at image location (x,y) Y, C_b, C_r for channels. The value of Equation (6) ranges between 16 and 240.

Therefore, the feature vector of the proposed system using 6 features is as follows

$$F = [F_R, F_G, F_B, F_Y, F_{C_b}, F_{C_r}] \quad (7)$$

3.2.4. Jaundice detection based on random forest

Random forest (RF), developed by Leo Breiman (Breiman 2001), is one of the highest reported performance classification methods (Miah et al. 2019). It can deal with continuous, binary, and categorical data. RF is a simple, fast, flexible, efficient and robust model which has numerous applications in different sectors such as banking, the stock market, e-commerce and medicine (Shaik and Srinivasan 2019). The RF algorithm is often considered for selecting an optimum and precise combination of the components and symptoms of a particular disease in the medical field (Zhang et al. 2018; Daunhawer et al. 2019; Trishna et al. 2019).

RF is classified as a supervised machine learning algorithm that is commonly used in regression and classification problems (Shaik and Srinivasan 2019). It develops decision trees on various samples and takes their average for regression and majority vote in case of classification, and thus the problem of overfitting is solved. It can deal with the data set containing categorical variables, as in the case of classification as well as continuous variables as in the case of regression. It achieves better outcomes for classification problems (Breiman 2001). Moreover, it can handle missing values. As the average answers given by many trees are taken, it is very stable and accurate (Shaik and Srinivasan 2019).

As shown in Figure 5, the following steps are involved in the RF algorithm (Ali et al. 2012):

Step 1: Let a data set contains k number of records. In RF, n number of random records will be considered from that data set.

Step 2: For each sample, individual decision trees will be created.

Step 3: An output will be produced by each decision tree.

Step 4: Final output will be considered using majority voting for classification or averaging for regression.

To classify jaundice or normal, we have used RF classification based on majority voting. We have considered an image dataset consisting of 511 images and two class labels: Jaundice and Normal. These images were used to train our model. After training, infant images were fed to the model for diagnosis.

If the output is jaundice, then the neonate requires UV therapy, and if the output is normal, then the neonate does not need any UV therapy.

4. Experimental results

Python 3.9 and MATLAB 2020a were used to implement our algorithm. To evaluate our automatic ROI selection technique, we have considered different scenarios, such as the infant in a straight position without a cap (Figure 3(a)), the infant with a tilted head (Figure 3(b)), and the infant in a straight position wearing cap (Figure 3(c)). It can be seen from Figure 3 that ROI was successfully selected automatically using our proposed technique. The red bounding boxes in Figure 3 represent the selected ROI in different cases.

A 10-fold cross-validation was performed to evaluate the ML algorithm selected for our jaundice detection system. We have considered an image dataset consisting of 511 images and two class labels: Normal and Jaundice. In the case of Stochastic Gradient Boosting, decision tree and random forest, number of trees = 100. In KNN, number of neighbours, k = 5.

The original dataset was randomly divided into 10 subsets of approximately equal size. Each subset is referred to as a fold. For each fold, the model was trained on the remaining 9 folds (the training set) and evaluated on the held-out fold (the validation set). The performance metric (e.g. accuracy, precision, recall, and F1 score) was calculated for each fold based on the predictions made by the model on the validation set. The process was repeated 10 times, with each fold serving as the validation set exactly once. The performance metrics obtained from each fold were averaged to get an overall assessment of the model's performance. The performance of the ML algorithm that had shown the best cross validation performance was used in our system.

The performance of different ML algorithms in terms of average accuracy, precision, recall, and F1-score are presented in Table 1. It can be seen from the table, that the performance of Random Forest shows the best cross validation performance with accuracy = 0.9922, precision = 0.9974, recall = 0.9920, and

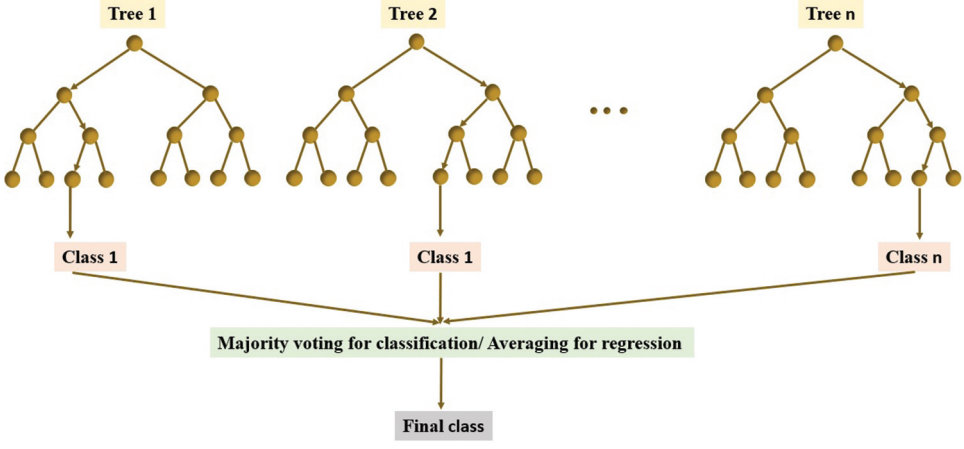

Figure 5. Representation of RF algorithm.

F1-score = 0.9946. Therefore, in our system we have used Random Forest algorithm.

The proposed system can be used to detect jaundice as well as to decide if the baby needs UV therapy or not using the RF algorithm based on skin colour analysis. A GUI panel using MATLAB software was designed for jaundice detection. The proposed MATLAB GUI panel (Figures 6–11) allows the operator, such as a nurse, doctor, or guardian, to open the image of the baby. Then, the algorithm was executed to identify jaundice based on skin colour and to determine whether the neonate needed UV therapy or not. The RGB histogram and their brightness values, skin state i.e. jaundice or normal, can be easily displayed through the proposed GUI panel.

Two different datasets were used to test the functionality of the proposed system. The first dataset was obtained by creating 20 images of 3D babies with varying skin tones. These images were used as an alternative to real babies to examine four different scenarios (Figures 6–9). Figure 6 represents a normal baby without jaundice in the GUI main panel of the proposed jaundice detection system. It can be seen from Figure 6 that the baby does not require UV therapy as the colour of his skin was normal without any yellowness. The GUI main panel of the proposed system for a baby with jaundice is shown in Figure 7, and it requires UV phototherapy as his skin is yellow. Figures 8 and 9 represent the brown skin infants with and without jaundice, respectively. The results for all 20 images of 3D babies are shown in Table 2.

The second data set comprises 30 images of babies (20 of these images are for healthy babies without jaundice, and the other 10 images are for babies with jaundice) downloaded from the internet. These images were captured by different cameras, with various skin tones, illumination conditions, and camera – infant distance. As represented in Table 3, the proposed jaundice detection system successfully identified all the babies without jaundice as 'Normal' and not needing UV therapy. Additionally, all the images of the babies who had jaundice were detected as 'Jaundice' and needed UV therapy. Figure 10 represents a baby who does not have jaundice as a result, does not need UV therapy. Figure 11 shows a baby who has jaundice and needs UV therapy.

The experimental result presents that the proposed jaundice detection system can be a potential non-invasive technique of jaundice detection in clinical applications.

Table 1. Comparison of the performance of different ML algorithms.

	Average Accuracy	Average Precision	Average Recall	Average F1 Score
Naïve Bayes	0.9120	.9917	0.8876	0.9359
KNN	0.9882	.9844	1	0.9921
SVM	0.9863	.9895	0.9920	0.9907
SGB	0.9882	.9947	0.9894	0.9919
Decision Tree	0.9903	.9974	0.9894	0.9933
Random Forest	**0.9922**	.9974	**0.9920**	**0.9946**

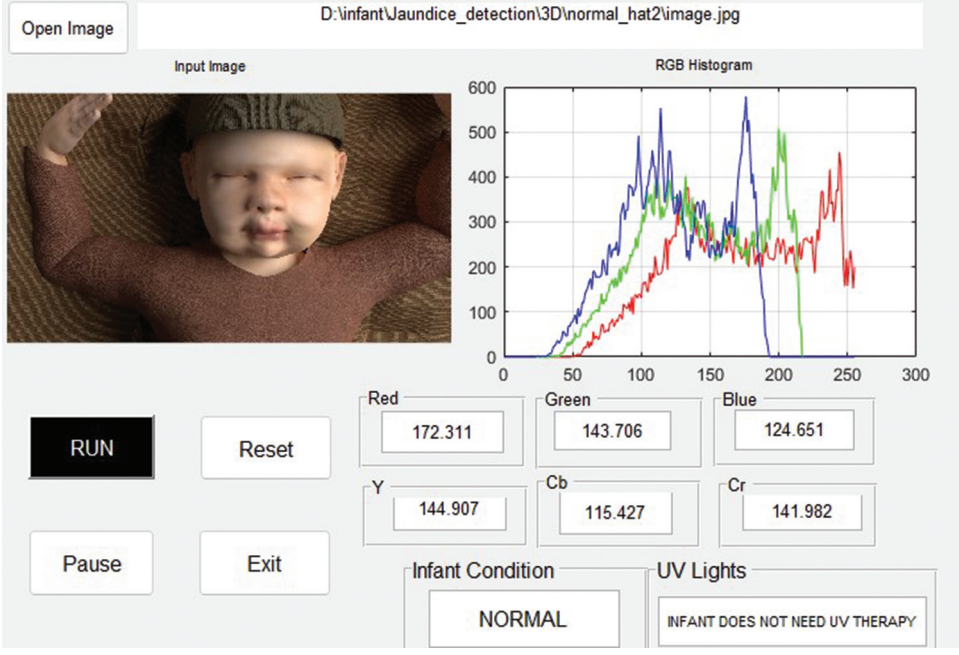

Figure 6. A 3D baby with light skin colour (jaundice-free).

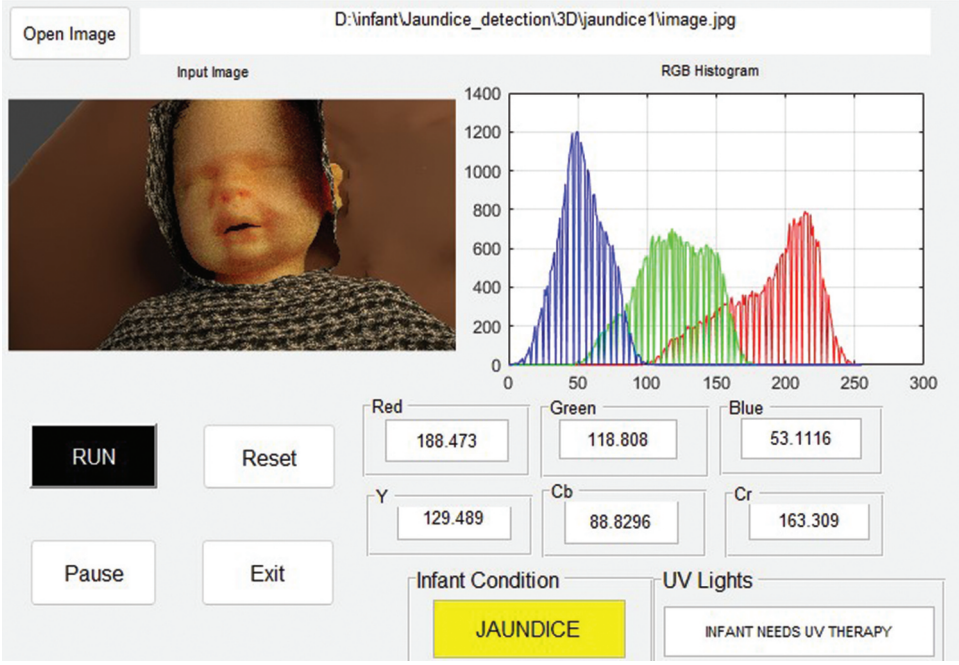

Figure 7. A 3D baby with a yellowish-light skin colour and jaundice.

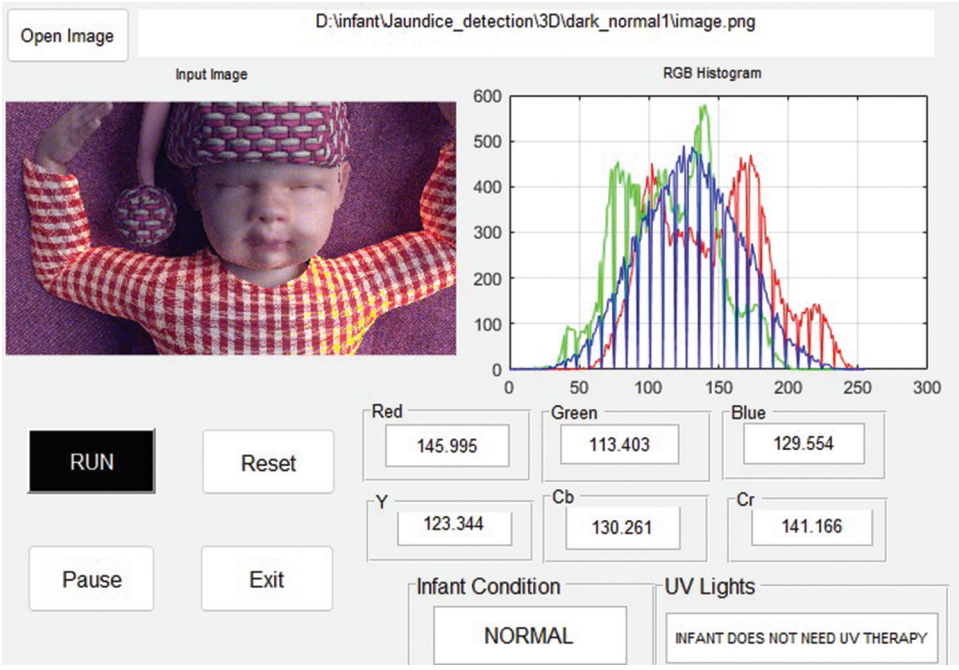

Figure 8. A 3D baby with brown skin colour and jaundice-free.

5. Discussion

There are several invasive and non-invasive techniques for detecting neonatal jaundice. However, existing invasive techniques are stressful, disruptive, and painful for the newborn, requiring skilled personnel and time. On the other hand, existing non-invasive devices are expensive. Therefore, we propose a non-invasive and non-contact neonatal jaundice detection system using a graphical user interface.

As shown in Table 4, most non-invasive systems in the literature used manual ROI selection (Rong et al. 2016; Juliastuti et al. 2019; Aune et al. 2020; Hashim et al. 2021). Fewer used automatic ROI selection techniques (Mansor et al. 2011; Kawano et al. 2018; Hashim et al. 2021); however, the existing ROI selection techniques detected the whole face which included areas such as mouth, eyes, nostrils, clothes, and background, which may affect the results of jaundice detection.

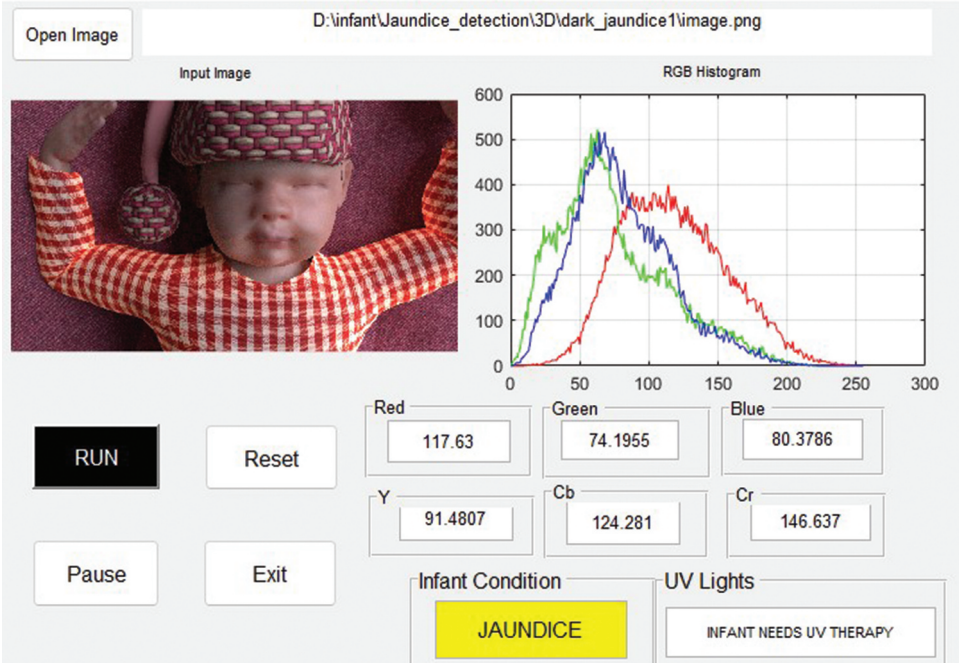

Figure 9. A 3D baby that has yellowish-brown skin and jaundice.

Jaundice detection is a real-time requirement, and the entire procedure becomes ineffective when the ROI selection is not automated. Moreover, the reliability of jaundice detection depends on selecting the correct skin ROI of the infant. Selecting the entire face might not be the best ROI as it can include undesirable areas such as the mouth, eyes, nostrils, clothes, and background. In the proposed method, we developed an automatic ROI selection technique and considered forehead as a ROI.

From Table 4, it can be seen that the proposed system compare favourable to the state-of-the art methods except Hashim et al. (2021) methods. However, they did skin colour analysis in RGB and YCbCr colour spaces to detect jaundice. The values of the B and Cb channels were compared with the predefined threshold value to determine whether the neonate had jaundice or not. In the proposed method, a machine learning algorithm based on RF was incorporated to classify jaundice or normal and determine whether the neonate requires treatment or not.

It is a good practice to denoise images or filter images with wavelet or GLCM (Vakharia et al. 2017; Patel et al. 2020). However, in the proposed system, we detected jaundice based on skin colour analysis. We calculated the mean values for each colour channel of RGB and YC_bCr colour spaces, which we considered as features for ML algorithms. The mean value of the brightness pixel for R, G, B, Y, C_b, Cr were measured. Therefore, it is not required to denoise images or filter images in our system.

As our proposed system is based on skin colour analysis and we used a digital camera, the system may have had

Table 2. Summary of 20 infants considered in the first dataset.

Infant	Red	Green	Blue	Y	C_b	C_r	Infant condition	UV Therapy
1	152.84	112.25	122.56	128.88	123.74	141.4	Normal	Does not need
2	175.64	129.19	141.6	140.11	126.57	147.50	Normal	Does not need
3	180.93	133.39	146.74	144.07	126.81	147.9	Normal	Does not need
4	199.67	167.62	145.77	166.04	113.71	143.62	Normal	Does not need
5	171.11	142.3	123.12	143.72	115.32	142.12	Normal	Does not need
6	203.02	170.5	148.13	168.59	113.42	143.86	Normal	Does not need
7	147.44	118.40	116.49	124.95	122.98	140.96	Normal	Does not need
8	145.99	113.40	129.5	123.34	130.26	141.16	Normal	Does not need
9.	172.31	143.70	124.65	144.90	115.42	141.98	Normal	Does not need
10.	193.59	153.81	148.06	157.42	119.87	146.09	Normal	Does not need
11.	117.63	74.19	80.37	91.48	104.28	146.63	Jaundice	Needs
12.	112.31	91.35	91.54	99.84	104.97	137.22	Jaundice	Needs
13.	188.47	118.80	53.11	129.48	88.82	163.31	Jaundice	Needs
14.	154.00	119.58	54.30	121.15	94.22	147.82	Jaundice	Needs
15.	140.75	105.36	53.94	110.54	100.17	147.21	Jaundice	Needs
16.	186.28	124.7	48.13	131.4	85.24	160.5	Jaundice	Needs
17.	193.48	144.45	75.3	145.88	90.23	154.48	Jaundice	Needs
18.	189.59	132.84	38.98	135.47	78.36	159.63	Jaundice	Needs
19.	205.05	131.17	58.28	140.4	85.03	165.5	Jaundice	Needs
20.	189.95	136.24	33.66	136.75	74.98	158.9	Jaundice	Needs

Table 3. Summary of 30 infants considered in the second dataset.

Infant	Red	Green	Blue	Y	C_b	C_r	Infant condition	UV Therapy
1.	199.5	165.67	37.10	154.38	66.54	37.10	Jaundice	Needs
2.	187.39	140.11	81.4	142.72	95.22	152.94	Jaundice	Needs
3.	144.17	104.17	52.22	110.66	99.3	149.27	Jaundice	Needs
4.	226.45	165.62	112.87	168.71	95.74	158.48	Jaundice	Needs
5.	141.24	82.75	58.46	99.72	108.60	155.38	Jaundice	Needs
6.	212.37	127.56	46.40	139.39	79.77	171.04	Jaundice	Needs
7.	214.11	134.76	88.25	147.60	95.72	166.10	Jaundice	Needs
8.	222.68	147.03	97.77	156.87	95.07	164.75	Jaundice	Needs
9.	191.00	132.32	75.45	139.15	94.28	157.85	Jaundice	Needs
10.	114.9	77.26	38.24	88.18	105.41	147.35	Jaundice	Needs
11.	209	153	116	158	103	155	Normal	Does not need
12.	229.97	194.98	171.73	190.17	112.52	145.17	Normal	Does not need
13.	243.89	189.17	157.49	189.40	105.94	154.29	Normal	Does not need
14.	230.02	177.53	164.28	180.65	114.51	152.10	Normal	Does not need
15.	212.46	177.35	170.40	176.67	119.78	143.97	Normal	Does not need
16.	232.37	206.21	194.91	198.72	119.14	140.21	Normal	Does not need
17.	197	167	156	166	119	142	Normal	Does not need
18.	242.72	225.85	220.57	213.80	123.21	135.72	Normal	Does not need
19.	224.52	186.06	155.34	182.65	108.86	147.13	Normal	Does not need
20.	192.22	137.46	116.53	146.07	110.84	153.84	Normal	Does not need
21.	212.52	153.52	119.74	159.72	104.51	156.33	Normal	Does not need
22.	238.21	200.51	188.17	196.68	117.13	145.41	Normal	Does not need
23.	242.76	219.26	210.94	209.50	120.80	139.07	Normal	Does not need
24.	223.17	195.58	186.15	190.15	119.86	140.83	Normal	Does not need
25.	204.05	138.62	123.67	150.39	111.58	157.81	Normal	Does not need
26.	205.10	160.10	144.00	163.474	114.4	148.82	Normal	Does not need
27.	233	218	211	206	123	136	Normal	Does not need
28.	226.25	205.78	206.58	198.05	125.32	136.97	Normal	Does not need
29.	239.55	185.57	169.12	187.60	112.85	152.87	Normal	Does not need
30.	244.78	194.99	180.06	194.79	113.99	151.02	Normal	Does not need

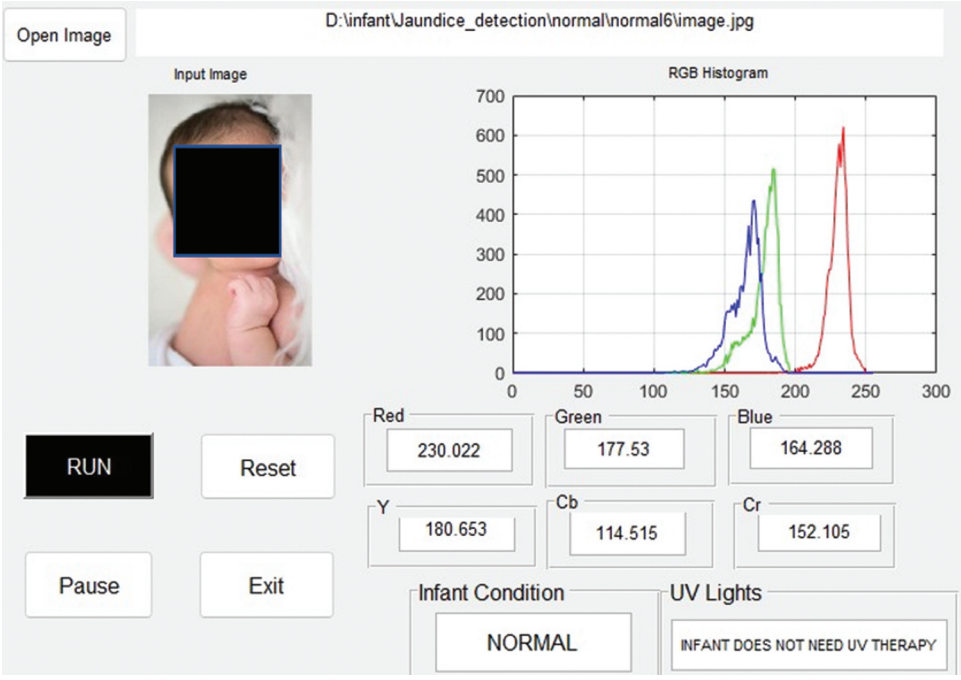

Figure 10. A normal baby without jaundice.

Table 4. Comparison with state-of-art methods.

Ref	ROI Selection	Jaundice detection	Detection rate of the system
Hashim et al.	Manual	Skin colour analysis in RGB and YC_bC_r colour spaces	100%
Rong et al.	Manual	Machine learning-based software	96%
Juliastuti et al.	Manual	Multivariable linear regression	90%
Hashim et al.	Automatic	Skin colour analysis in RGB and YC_bC_r colour spaces	100%
Mansor et al.	Automatic	k-NN	95.6%
Proposed method	**Automatic**	**Machine learning based on RF**	**100%**

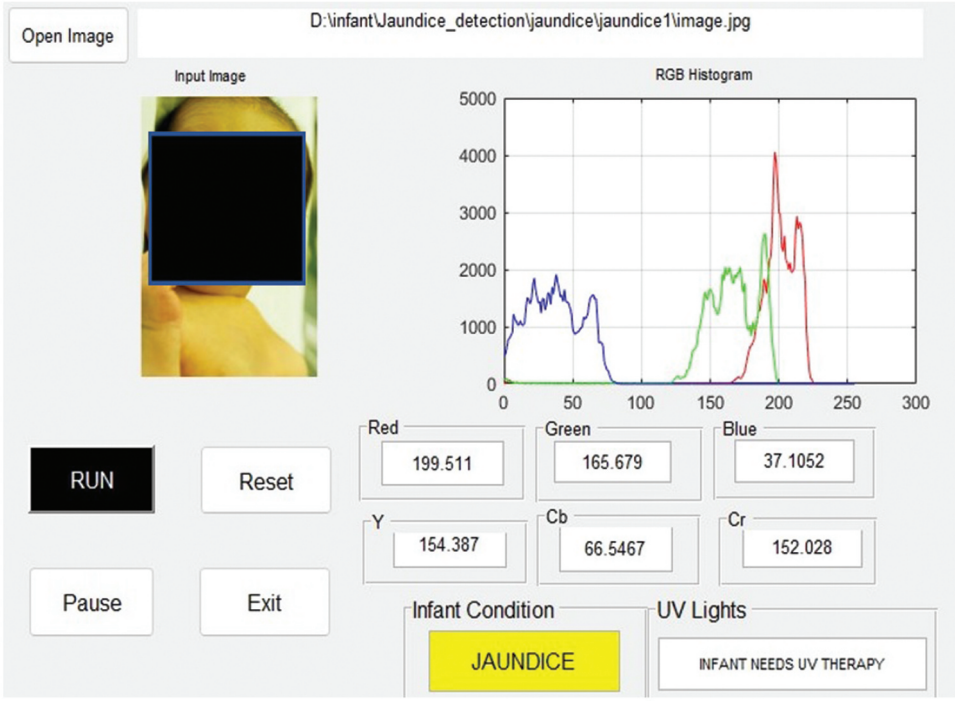

Figure 11. A baby with a yellowish skin colour who has jaundice.

limitations for babies with different skin tones and under different lighting conditions. To minimise these challenges, we fed the random forest with variations of these two parameters, showing that the proposed system could detect jaundice across a wide range of skin tones and lighting conditions.

6. Conclusion

In this paper, a non-invasive and easy-to-use system was developed to monitor neonatal jaundice by taking images of babies and using a graphical user interface. In the proposed system, first, we have designed an automatic ROI selection technique including face detection, face landmark detection and ROI i.e. forehead selection. Then, the skin colour of the selected forehead region was analysed in both RGB and YC_bC_r colour spaces. Finally, jaundice has been detected using a machine learning algorithm based on RF. Moreover, the system can notify whether the neonates require phototherapy or not.

The experimental results show that the proposed jaundice detection technique can be a potential alternative to the existing procedures that involve blood samples using syringes and needles. It lessens the stress, trauma, and pain involved in conventional invasive methods. Moreover, it gives the result within a few minutes without the involvement of any highly qualified personnel. It is also a cost-effective, affordable, and easy-to-use tool that is appropriate for monitoring an infant in the comfort of their own residence. Moreover, it is advantageous in emergency situations where the availability of specialised disease diagnosis is missing. However, in the proposed system, we have used images of 3D babies and images of babies from the internet. Therefore, we do not have any gold-standard data to validate. Besides, babies need to be in a frontal position in the images, as we used a frontal face detector. In the future, we plan to use real-time baby images with gold-standard clinical data to make the system feasible for real-time applications.

Disclosure statement

No potential conflict of interest was reported by the author(s).

Funding

This research is funded by Research Training Program domestic (RTPd) scholarship provided by the University of South Australia on behalf of the Australian Commonwealth Department of Education and Training.

References

Ali J, Khan R, Ahmad N, Maqsood I. 2012. Random forests and decision trees. Int J Comput Sci Iss (IJCSI). 9(5):272.

Amani M, Falk H, Jensen OD, Vartdal G, Aune A, Lindseth F. 2019. Color calibration on human skin images. International Conference on Computer Vision Systems, Thessaloniki, Greece. Cham: Springer.

Angelico R, Liccardo D, Paoletti M, Pietrobattista A, Basso MS, Mosca A, Safarikia S, Grimaldi C, Saffioti MC, Candusso M. 2021. A novel mobile phone application for infant stool color recognition: an easy and effective tool to identify acholic stools in newborns. J Med Screen. 28 (3):230–237. doi: 10.1177/0969141320974413.

Ansong-Assoku B, Ankola PA. 2018. Neonatal Jaundice. Neonatal jaund.

Aune A, Vartdal G, Bergseng H, Randeberg LL, Darj E. 2020. Bilirubin estimates from smartphone images of newborn infants' skin correlated highly to serum bilirubin levels. Acta Paediatr. 109(12):2532–2538. doi: 10.1111/apa.15287.

Aydın M, Hardalaç F, Ural B, Karap S. 2016. Neonatal jaundice detection system. J Med Syst. 40(7):1–11. doi: 10.1007/s10916-016-0523-4.

Bishop CM, Nasrabadi NM. 2006. Pattern recognition and machine learning. Vol. 4. Newyork: Springer; p. 4.
Breiman L. 2001. Random forests. Mach Learn. 45(1):5–32. doi: 10.1023/A:1010933404324.
Castro-Ramos J, Toxqui-Quitl C, Manriquez FV, Orozco-Guillen E, Padilla-Vivanco A, Sánchez-Escobar JJ. 2014. Detecting jaundice by using digital image processing. Three-Dimensional and Multidimensional Microscopy: Image Acquisition and Processing XXI; SPIE.
Chakraborty A, Goud S, Shetty V, Bhattacharyya B. 2020. Neonatal jaundice detection system using CNN algorithm and image processing. Int J Electric Engg Technol. 11(3):248–264.
Chee Y, Chung P, Wong R, Wong K. 2018. Jaundice in infants and children: causes, diagnosis, and management. Hong Kong Med J. 24(3):285–292. doi: 10.12809/hkmj187245.
Chen J, Stanley RJ, Moss RH, Van Stoecker W. 2003. Colour analysis of skin lesion regions for melanoma discrimination in clinical images. Skin Res Technol. 9(2):94–104. doi: 10.1034/j.1600-0846.2003.00024.x.
Daunhawer I, Kasser S, Koch G, Sieber L, Cakal H, Tütsch J, Pfister M, Wellmann S, Vogt JE. 2019. Enhanced early prediction of clinically relevant neonatal hyperbilirubinemia with machine learning. Pediatr Res. 86 (1):122–127. doi: 10.1038/s41390-019-0384-x.
Deepthi AR, Singh C, Jeeva JB. 2019. A Device to Detect Hyperbilirubin through Non-Invasive Technique. 2019 Innovations in Power and Advanced Computing Technologies (i-PACT), Vellore, India. IEEE.
De Greef L, Goel M, Seo MJ, Larson EC, Stout JW, Taylor JA, Patel SN. 2014. Bilicam: using mobile phones to monitor newborn jaundice. Proceedings of the 2014 ACM International Joint Conference on Pervasive and Ubiquitous Computing. SEATTLE, WA, USA: ACM Digital Library.
Dzulkifli FA, Mashor MY, Khalid K. 2018. Methods for determining bilirubin level in neonatal jaundice screening and monitoring: a literature review. J Eng Res Educ. 10:1–10.
Friedman JH. 2020. Contrast trees and distribution boosting. Proc Natl Acad Sci USA. 117(35):21175–21184. doi: 10.1073/pnas.1921562117.
Gartner LM. 1994. Neonatal jaundice. Pediatr Rev. 15(11):422–432. doi: 10.1542/pir.15.11.422.
Gupta A, Kumar A, Khera P. 2015. Method and model for jaundice prediction through non-invasive bilirubin detection technique. Int J Eng Res Technol. 4(8):34–38. doi: 10.17577/IJERTV4IS080149.
Han J, Kamber M, Pei J. 2012. Data mining concepts and techniques third edition. University of Illinois at Urbana-Champaign Micheline Kamber Jian Pei Simon Fraser University.
Hashim W, Alkhaled M, Al-Naji A, Al-Rayahi I. 2021. A review on image processing based neonatal jaundice detection techniques. 2021 7th International Conference on Contemporary Information Technology and Mathematics (ICCITM), Mosul, Iraq. IEEE.
Hashim W, Al-Naji A, Al-Rayahi IA, Alkhaled M, Chahl J. 2021. Neonatal jaundice detection using a computer vision system. Designs. 5(4):63. doi: 10.3390/designs5040063.
Hashim W, Al-Naji A, Al-Rayahi IA, Oudah M. 2021. Computer vision for jaundice detection in neonates using graphic user interface. IOP Conference Series: Materials Science and Engineering, Baghdad, Iraq. IOP Publishing.
Hastie T, Tibshirani R, Friedman JH. 2009. The elements of statistical learning: data mining, inference, and predictionVol. 2. Springer. doi: 10.1007/978-0-387-84858-7.
Juliastuti E, Nadhira V, Satwika YW, Aziz NA, Zahra N. 2019. Risk zone estimation of newborn jaundice based on skin color image analysis. 2019 6th International Conference on Instrumentation, Control, and Automation (ICA), Bandung, Indonesia. IEEE.
Kakumanu P, Makrogiannis S, Bourbakis N. 2007. A survey of skin-color modeling and detection methods. Pattern Recogn. 40(3):1106–1122. doi: 10.1016/j.patcog.2006.06.010.
Katti B, Babu BS. 2021. Analytical review on the technologies designed for the better detection and treatment of neonatal jaundice. Int Res J Engg Technol (IRJET). 8(6):2395–0056.
Kawano S, Zin TT, Kodama Y. 2018. A study on non-contact and non-invasive neonatal jaundice detection and bilirubin value prediction. 2018 IEEE 7th Global Conference on Consumer Electronics (GCCE), Nara, Japan. IEEE.
Keren R, Tremont K, Luan X, Cnaan A. 2009. Visual assessment of jaundice in term and late preterm infants. Arch Dis Childhood-Fetal Neonatal Ed. 94 (5):F317–F322. doi: 10.1136/adc.2008.150714.
Khanam FTZ, Al-Naji A, Perera AG, Gibson K, Chahl J. 2022. Non-contact automatic vital signs monitoring of neonates in NICU using video camera imaging. Comput Methods Biomechan Biomed Engg: Imag visualizat. 11(2):278–285. doi: 10.1080/21681163.2022.2069598.
King DE. 2009. Dlib-ml: a machine learning toolkit. J Mach Learn Res. 10:1755–1758.
Kumar RV, Raju KP, Kumar LR, Kumar M. 2016. Gray level to RGB using YcbCr color space technique. Int J Comput Appl. 147(7):25–28. doi: 10.5120/ijca2016911180.
Laddi A, Kumar S, Sharma S, Kumar A. 2013. Non-invasive jaundice detection using machine vision. IETE J Res. 59(5):591–596. doi: 10.4103/0377-2063.123765.
Maisels MJ. 2015. Managing the jaundiced newborn: a persistent challenge. Cmaj. 187(5):335–343. doi: 10.1503/cmaj.122117.
Mansor MN, Yaacob S, Muthusamy H, Nisha S. 2011. PCA-based feature extraction and k-NN algorithm for early jaundice detection. System. 1 (1):25–29.
Mansouri M, Mahmoodnejad A, Taghizadeh Sarvestani R, Gharibi F. 2015. A comparison between transcutaneous bilirubin (TcB) and total serum bilirubin (TSB) measurements in term neonates. Int J Pediatr. 3 (3.1):633–641.
Miah MM, Tazim RJ, Johora FT, Al Imran MI, Surma SS, Islam F, Shabab R, Shahnaz C, Subhana A. 2019. Non-invasive bilirubin level quantification and jaundice detection by sclera image processing. 2019 IEEE Global Humanitarian Technology Conference (GHTC), Seattle, WA, USA. IEEE.
Mitchell TM. 2007. Machine learning. Vol. 1. McGraw-hill New York.
Mreihil K, Benth JŠ, Stensvold HJ, Nakstad B, Hansen TWR, Group NNPS, Network NN, Scheck O, Nordin S, Prytz A. 2018. Phototherapy is commonly used for neonatal jaundice but greater control is needed to avoid toxicity in the most vulnerable infants. Acta Paediatr. 107(4):611–619. doi: 10.1111/apa.14141.
Mreihil K, Nakstad B, Stensvold HJ, Benth JŠ, Hansen TWR. 2018. Uniform national guidelines do not prevent wide variations in the clinical application of phototherapy for neonatal jaundice. Acta Paediatr. 107 (4):620–627. doi: 10.1111/apa.14142.
mTkalcic M, Tasic F. 2002. Project for the digital signal processing course. University of Ljubljana Colour spaces.
Mussavi M, Niknafs P, Bijari B. 2013. Determining the correlation and accuracy of three methods of measuring neonatal bilirubin concentration. Iran J Pediatr. 23(3):333.
Osman Z, Ahmad A, Muharam A. 2014. Rapid prototyping of neonatal jaundice detector using skin optics theory. 2014 IEEE Conference on Biomedical Engineering and Sciences (IECBES), Kuala Lumpur, Malaysia. IEEE.
Padidar P, Shaker M, Amoozgar H, Khorraminejad-Shirazi M, Hemmati F, Najib KS, Pourarian S. 2019. Detection of neonatal jaundice by using an android OS-based smartphone application. Iran J Pediatr. 29(2). doi: 10.5812/ijp.84397.
Patel DR, Thakker H, Kiran M, Vakharia V. 2020. Surface roughness prediction of machined components using gray level co-occurrence matrix and bagging tree. FME Trans. 48(2):468–475. doi: 10.5937/fme2002468P.
Puppalwar P. 2012. Review on "evolution of methods of bilirubin estimation". IOSR J Dental Med Sci. 1(3):17–28. doi: 10.9790/0853-0131728.
Rennie J, Burman-Roy S, Murphy MS. 2010. Neonatal jaundice: summary of NICE guidance. Bmj. 340.
Riskin A, Tamir A, Kugelman A, Hemo M, Bader D. 2008. Is visual assessment of jaundice reliable as a screening tool to detect significant neonatal hyperbilirubinemia? J Pediatr. 152(6):782–787. doi: 10.1016/j.jpeds.2007.11.003.
Rong Z, Luo F, Ma L, Chen L, Wu L, Liu W, Du L, Luo X. 2016. Evaluation of an automatic image-based screening technique for neonatal hyperbilirubinemia. Zhonghua Er Ke Za Zhi= Chinese J Pediatr. 54 (8):597–600. doi: 10.3760/cma.j.issn.0578-1310.2016.08.008.
Shafiq MF, Ahmed Z, Ahmad AM. 2019. Validity of visual assessment of neonatal jaundice for screening significant hyperbilirubinaemia. PAFMJ. 69(1):212–216.

Shaik AB, Srinivasan S. 2019. A brief survey on random forest ensembles in classification model. International Conference on Innovative Computing and Communications, Ostrava, Czech Republic. Springer.

Singla R, Singh S. 2016. A framework for detection of jaundice in new born babies using homomorphic filtering based image processing. 2016 International Conference on Inventive Computation Technologies (ICICT), Coimbatore, India. IEEE.

Srividya K, Renganathan K, Meha S, Yogabhuvaneswari U. 2022. Review on jaundice detection in neonates using image processing. 2022 International Conference on Communication, Computing and Internet of Things (IC3IoT), Chennai, India. IEEE.

Tkalcic M, Tasic JF. 2003. Colour spaces: perceptual, historical and applicational background. Vol. 1. Ljubljana, Slovenia: IEEE.

Trishna EP, Sharma SK. 2019. Detection of hepatitis (a, b, c and e) viruses based on random forest, k-nearest and naive Bayes classifier. 2019 10th International Conference on Computing, Communication and Networking Technologies (ICCCNT), Kanpur, India. IEEE.

Ullah S, Rahman K, Hedayati M. 2016. Hyperbilirubinemia in neonates: types, causes, clinical examinations, preventive measures and treatments: a narrative review article. Iran J Public Health. 45(5):558.

Vakharia V, Kiran MB, Dave NJ, Kagathara U. 2017. Feature extraction and classification of machined component texture images using wavelet and artificial intelligence techniques. 2017 8th International Conference on Mechanical and Aerospace Engineering (ICMAE), Prague, Czech Republic. IEEE.

Vezhnevets V, Sazonov V, Andreeva A. 2003. A survey on pixel-based skin color detection techniques. Proceedings of Graphicon; Russia: Moscow.

Viola P, Jones MJ. 2004. Robust real-time face detection. Int J Comput Vis. 57(2):137–154. doi: 10.1023/B:VISI.0000013087.49260.fb.

Women's NCCf, Health Cs. 2010. Neonatal jaundice: clinical guideline. London (UK): National Institute for Health and Clinical Excellence (NICE).

Zhang Z, Li N, Gao H, Cai Z, Si S, Geng Z. 2018. Preoperative analysis for clinical features of unsuspected gallbladder cancer based on random forest. 2018 IEEE International Conference on Industrial Engineering and Engineering Management (IEEM), Bangkok, Thailand. IEEE.